nature climate change

LETTERS

PUBLISHED ONLINE: 23 MAY 2016 | DOI: 10.1038/NCLIMATE3036

The climate response to five trillion tonnes of carbon

Katarzyna B. Tokarska[1]*, Nathan P. Gillett[2], Andrew J. Weaver[1], Vivek K. Arora[2] and Michael Eby[1,3]

Concrete actions to curtail greenhouse gas emissions have so far been limited on a global scale[1], and therefore the ultimate magnitude of climate change in the absence of further mitigation is an important consideration for climate policy[2]. Estimates of fossil fuel reserves and resources are highly uncertain, and the amount used under a business-as-usual scenario would depend on prevailing economic and technological conditions. In the absence of global mitigation actions, five trillion tonnes of carbon (5 EgC), corresponding to the lower end of the range of estimates of the total fossil fuel resource[3], is often cited as an estimate of total cumulative emissions[4–6]. An approximately linear relationship between global warming and cumulative CO_2 emissions is known to hold up to 2 EgC emissions on decadal to centennial timescales[7–11]; however, in some simple climate models the predicted warming at higher cumulative emissions is less than that predicted by such a linear relationship[8]. Here, using simulations[12] from four comprehensive Earth system models[13], we demonstrate that CO_2-attributable warming continues to increase approximately linearly up to 5 EgC emissions. These models simulate, in response to 5 EgC of CO_2 emissions, global mean warming of 6.4–9.5 °C, mean Arctic warming of 14.7–19.5 °C, and mean regional precipitation increases by more than a factor of four. These results indicate that the unregulated exploitation of the fossil fuel resource could ultimately result in considerably more profound climate changes than previously suggested.

We analyse prescribed-concentration simulations from the Fifth Coupled Climate Model Intercomparison Project (CMIP5)[13] driven by the Representative Concentration Pathway 8.5 Extension scenario (RCP 8.5-Ext[12]; see Methods), which represents a scenario of strongly increasing greenhouse gas concentrations in the absence of climate mitigation policies, leading to a stabilization at a radiative forcing level of 12 W m^{-2} by year 2300[7,12] (see Methods). We use all four Earth system models (ESMs; BCC-CSM 1.1, HadGEM2-ES, IPSL-CM5A-LR and MPI-ESM-LR), which carried out the RCP 8.5-Ext simulations and for which the data required to calculate cumulative emissions were available (see Methods). In addition, we compare the results with seven Earth system models of intermediate complexity (EMICs) that carried out RCP 8.5-Ext simulations[14]. Although the RCP 8.5-Ext simulations extend well outside the range of conditions for which the models' parameterizations could be validated against reality, these parameterizations are based on physical, chemical and biological principles, and our sampling over multiple models accounts, in part, for uncertainties associated with differences in the representation of the physical climate system and carbon cycle between models[15,16].

The four CMIP5 models simulate global mean surface temperature increases of between 8.1 and 11.5 °C for the period 2281–2300 relative to 1986–2005 in the RCP 8.5-Ext scenario (Fig. 1a). These increases are towards the upper end of the 4.9–10.7 °C (5–95% confidence interval; ref. 7 Table 12.2) range given for the full ensemble of CMIP5 models that carried out these simulations[7], and generally above increases of between 3.8 and 8.9 °C simulated by seven EMICs in 2300[14] (Fig. 1a and Supplementary Fig. 1a). The fluxes of carbon into both land and ocean exhibit progressive increases in all models until the mid-twenty-first century, followed by a gradual decline in the atmosphere–land and atmosphere–ocean fluxes during the 2100–2300 period, despite the continuously increasing atmospheric CO_2 concentrations (Fig. 1b,c, respectively), consistent with previous findings[14,17].

Time-integrated carbon fluxes, representing the atmospheric, land and ocean carbon reservoir evolution over time, are shown in Fig. 2. The land continues to take up carbon until 2100 owing to the CO_2 fertilization effect at high CO_2 concentration (Fig. 2a). Subsequently, a decline in terrestrial carbon storage occurs during the period 2100–2300 for MPI-ESM-LR and IPSL-CM5A-LR, most likely due to an increase in heterotrophic respiration larger than that in net primary productivity, as the CO_2 fertilization effect saturates at higher CO_2 levels and higher temperature levels limit photosynthesis, especially in tropical regions[14,18,19] (Fig. 2a). In MPI-ESM-LR and IPSL-SM5A-LR total land carbon is close to pre-industrial levels in 2300 despite the CO_2 concentration of 1,962 ppm, owing to pronounced carbon–climate feedbacks[15]. The land carbon pool stabilizes but does not strongly decline for HadGEM2-ES and BCC-CSM 1.1. The land carbon uptake would be expected to be weaker if the models included nutrient constraints on photosynthesis[16], permafrost feedbacks[20], or some representation of downregulation of photosynthesis with increasing CO_2[21]. For all of the models, the ocean continues to take up carbon to the year 2300, albeit at a decreasing rate of uptake than after 2100 (Fig. 2b). Although there are significant differences in the regional pattern of land carbon uptake response, the regions of highest carbon uptake in year 2100 generally occur in the northern high latitudes, while much of the tropics releases carbon to the atmosphere (Supplementary Fig. 2a). The regional responses intensify at 5 EgC of carbon released, compared with 2100 (Supplementary Fig. 2b), indicating even more outgassing in the tropics due to unfavourably high temperatures negatively affecting vegetation growth and more uptake in the northern high latitudes, probably driven by more vegetation growth due to warmer temperatures in that region.

Cumulative CO_2 emissions, diagnosed from the sum of changes in atmospheric CO_2 burden and time-integrated atmosphere–land

[1]School of Earth and Ocean Sciences, University of Victoria, 3800 Finnerty Road, Victoria, British Columbia V8W 3V6, Canada. [2]Canadian Centre for Climate Modelling and Analysis, Environment and Climate Change Canada, University of Victoria, PO Box 1700, STN CSC, Victoria, British Columbia V8W 2Y2, Canada. [3]Department of Geography, Simon Fraser University, Burnaby, British Columbia V5A 1S6, Canada. *e-mail: tokarska@uvic.ca

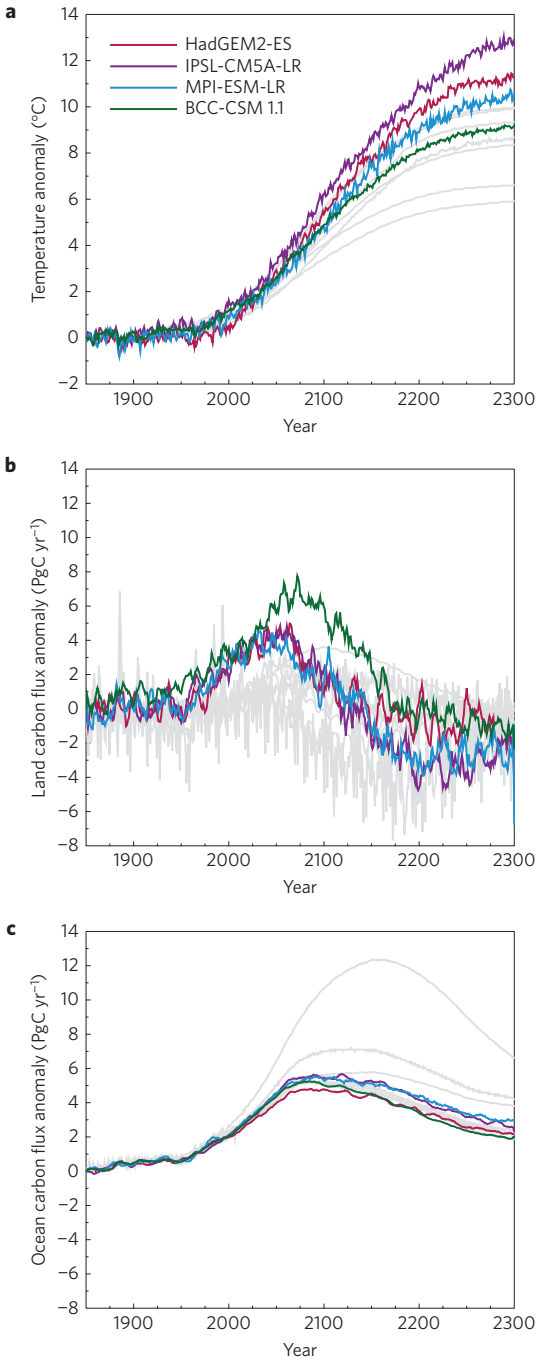

Figure 1 | Global mean temperature and carbon fluxes simulated in the RCP 8.5-Ext simulations. a–c, Global mean near-surface temperature anomaly (**a**), atmosphere–land carbon flux anomaly (**b**), and atmosphere–ocean carbon flux anomaly (**c**). Anomalies are calculated with respect to the corresponding year in the pre-industrial control simulation to remove the effects of any drift. The carbon fluxes (**b**,**c**) are ten-year running means. Grey lines indicate EMIC responses for comparison.

and atmosphere–ocean carbon fluxes[7], are shown in Fig. 2d (Supplementary Fig. 1b for EMICs). Total cumulative emissions increase strongly up to 2200, followed by approximate stabilization around 5 EgC by 2300 (Fig. 2d), associated with stabilization of atmospheric CO_2 concentration (Fig. 2c).

Figure 3 shows the relationship between temperature change and cumulative emissions for the four CMIP5 ESMs (Fig. 3a) and the seven EMICs considered (Fig. 3c). The RCP8.5-Ext simulations are not driven exclusively by changes in CO_2 concentration, but also include changes in other greenhouse gases and aerosols. The non-CO_2 forcing (such as that due to CH_4, N_2O, halocarbons and aerosols) is approximately constant during the period 2100–2300 and CO_2 is the dominant forcing in the RCP 8.5-Ext scenario: the ratio of CO_2 to total radiative forcing is 79% in 2100 and 85% in 2300 (Supplementary Fig. 3). To approximate the response to CO_2 changes alone, temperature changes in Fig. 3a,c are hence scaled by the ratio of CO_2 radiative forcing to total radiative forcing for each year. Particularly in the period after 2100, on which we focus here, this is likely to be a good approximation, because the ratio of CO_2 to total forcing is approximately constant over this period, so differences in the time profile of forcing and response are not important, and aerosol and ozone forcing are close to zero over this period. Hence, the ratio of CO_2 to total forcing is determined by the radiative forcings of the well-mixed greenhouse gases, which are well constrained and not strongly model dependent (Supplementary Fig. 3). Figure 3a,c also compares RCP 8.5-Ext simulations with simulations in which CO_2 increases at a rate of 1% yr^{-1} and all other forcings stay at their pre-industrial levels (1PCTCO$_2$, Fig. 3a[10], dotted lines). Note that the sharp increase in temperature as a function of cumulative emissions at the end of the IPSL-CM5A-LR and MPI-ESM-LR simulations in Fig. 3a results from ongoing warming (Fig. 1a) during a period in which cumulative emissions are approximately constant (Fig. 2d), a feature previously seen in some[8,22], but not all[23], other models. Figure 3a shows that the warming in the RCP 8.5-Ext simulations scaled by the ratio of CO_2 to total forcing, for a given magnitude of cumulative emissions, is slightly higher than for the 1PCTCO$_2$ simulations. One possible reason for this is the warming from non-CO_2 greenhouse gases, which reduces the diagnosed cumulative emissions in the RCP 8.5-Ext simulations[7,24] associated with the carbon–climate feedback. Nonetheless, Fig. 3a suggests that the ratio of warming to cumulative emissions continues to behave approximately linearly even up to cumulative emissions of 5 EgC. We verified this result by estimating the global warming due to CO_2 only at 5 EgC emissions for each of the four ESMs that ran the full RCP 8.5-Ext simulations (see Methods). This warming was used to calculate the ratio of CO_2-attributable warming to emissions at 5 EgC ($TCRE_{5EgC}$), which was compared with the ratio of warming to emissions at doubled pre-industrial CO_2 (approximately 1.4 EgC emissions) in the 1PCTCO$_2$ simulations[10] (TCRE) (Fig. 3b). Although there is variation in the ratio of warming to cumulative emissions for individual models, with the IPSL-CM5A-LR model showing a higher ratio at 5 EgC and the BCC-CSM 1.1 model a lower ratio, overall the mean ratio of warming to emissions across the four models was very similar at 5 EgC (1.63 °C EgC^{-1}) to the ratio of warming to emissions at approximately 1.40 EgC (1.67 °C EgC^{-1})[10]. Thus, overall in these ESMs, there is no evidence of the pronounced decrease in the ratio of CO_2-attributable warming to emissions at high emission levels seen in simple climate carbon models[8] and some EMICs[14].

A comparison of these results with simulations from a range of EMICs[14,18] indicates that all seven EMICs considered have a $TCRE_{5EgC}$ that is lower than their TCRE (Fig. 3d), and that departures from a linear relationship between warming and cumulative emissions are on average larger for the EMICs than for the ESMs (Supplementary Fig. 4). Supplementary Fig. 5 demonstrates that the ratio of $TCRE_{5EgC}$ to TCRE is linearly related to the ratio of warming at four times pre-industrial CO_2 to double pre-industrial CO_2 in a 1PCTCO$_2$ simulation across the ensemble of ESMs and EMICs we consider, and that this warming ratio is substantially greater than two in all four ESMs we consider[25]. Moreover, the two EMICs, which do not contain a three-dimensional ocean model (UMD and DCESS), are outliers both in terms of having a low warming ratio, and a low ratio of $TCRE_{5EgC}$ to TCRE (Supplementary Fig. 5),

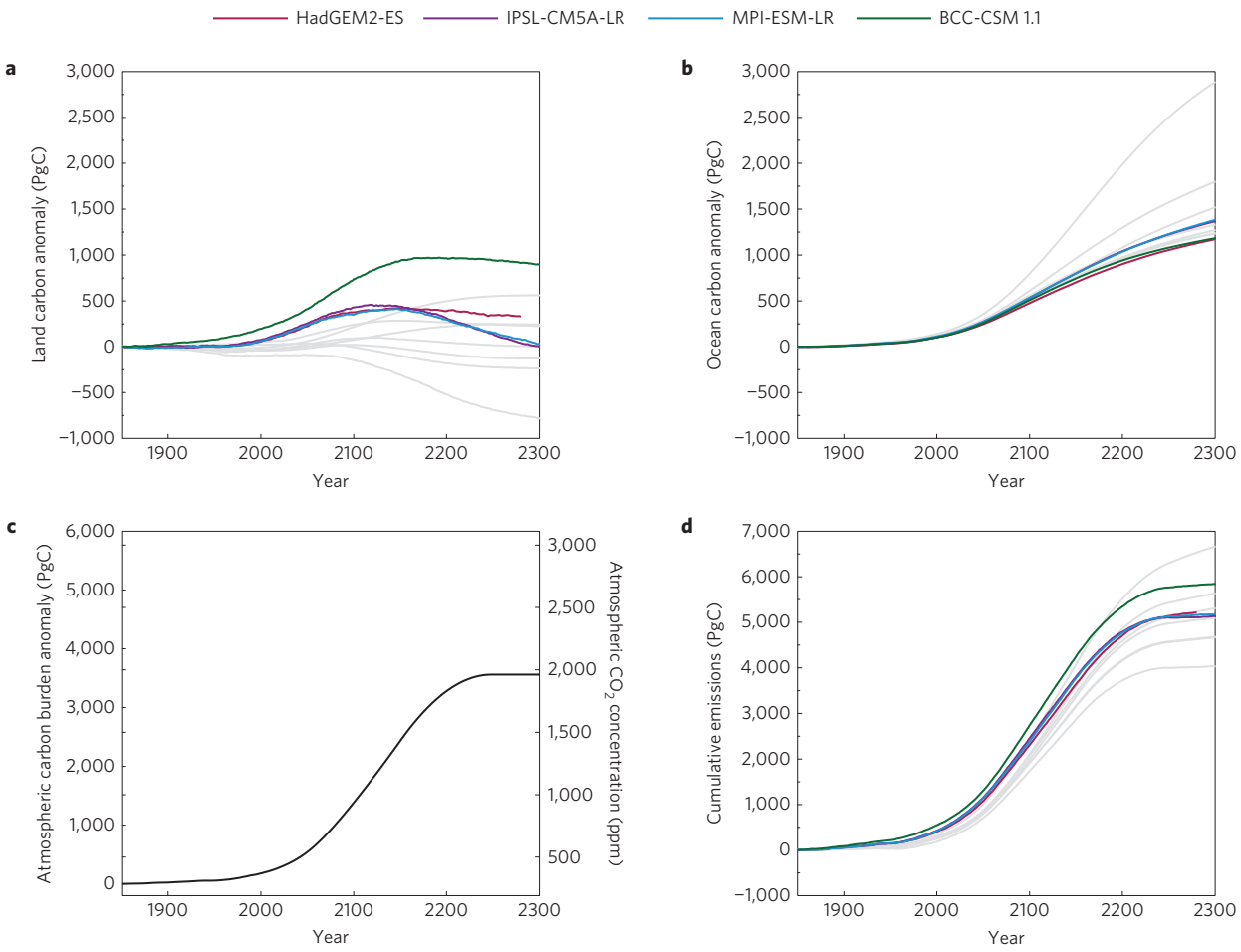

Figure 2 | Carbon budget quantities. a,**b**, Cumulative atmosphere–land (**a**) and atmosphere–ocean (**b**) CO_2 fluxes for the period 1850–2300, after taking into account any drift in the pre-industrial control simulation. **c**, Changes in prescribed atmospheric carbon burden for the historical (1850–2005), RCP 8.5 (2006–2100) and RCP 8.5-Ext (2101–2300) scenarios. **d**, Cumulative CO_2 emissions consistent with the prescribed CO_2 pathway in **c** as simulated by the four ESMs diagnosed as a sum of **a**–**c**. Grey lines show EMIC responses for comparison.

consistent with previous work indicating that the enhancement of warming per unit forcing at higher forcing levels in CMIP5 ESMs is primarily a result of weakening heat fluxes into the deep ocean[25], which are unlikely to be well represented in these models. Consistent with our suggestion that differences in ocean heat uptake are important, there are systematic differences in the fraction of realized warming in the EMICs we consider and the CMIP5 ESMs in a 1PCTCO$_2$ simulation, which have been attributed to differences in the profile of ocean heat uptake between the two classes of models[22]. It has previously been suggested that at high emissions the logarithmic dependence of the radiative forcing on the CO_2 concentration is likely to dominate increases in the airborne fraction of CO_2 at high cumulative emissions to give a decrease in the ratio of warming to emissions[7,10]. Our results, however, suggest that in these CMIP5 ESMs decreasing atmosphere–ocean heat fluxes[25] combined with positive carbon–climate feedbacks, which increase the cumulative airborne fraction (Supplementary Fig. 6), compensate for the radiative forcing effect to keep this ratio approximately linear even at high cumulative emissions. Besides the role of a stronger decrease in the efficiency of ocean heat uptake with warming in the ESMs compared with the EMICs[22,25], a more rapid than logarithmic increase in CO_2 radiative forcing or a decline in climate feedback parameter at higher warming levels in the ESMs[25] could also contribute to driving their relatively higher levels of warming at high cumulative emissions. Additional simulations would be required to test and distinguish these hypotheses.

Simulated CO_2-attributable global mean warming in response to 5 EgC emissions, a representative estimate of eventual carbon emissions in the absence of any climate change mitigation policy, ranges from 6.4 to 9.5 °C across four ESMs, with a mean of 8.2 °C (Supplementary Data Table 1). This warming estimate is higher than that predicted in previous studies based on simpler models[8,14]. A Monte Carlo estimate based on a simple carbon–climate model tuned to reproduce the behaviour of the C4MIP models at low cumulative emissions predicted most likely warming of about 5 °C for 5 EgC emitted to the atmosphere[8]. An EMIC inter-comparison study reports a model-mean global mean warming of 7.8 °C (ranging from 4.7 to 9.8 °C) for the RCP 8.5 scenario in the year 3000 relative to 1986–2005, where the diagnosed cumulative emissions range from approximately 4.3 EgC to 11.3 EgC relative to the same base period[14], and a warming of 8.9 °C was simulated in response to 5.3 EgC emissions, by the UVic EMIC[26].

We note that the four CMIP5 models we consider exhibit warming in 2281–2300 under RCP 8.5-Ext towards the upper end of the CMIP5 range, and their TCREs are all above the best estimate from observations (Fig. 3b). However, if we discount the simulated warming from HadGEM2-ES on the basis that its TCRE is outside the estimated 5–95% range estimated from observations (Fig. 3b), the warming range at 5 EgC from the remaining three models, whose TCREs are well within the observationally constrained range, is unchanged. If suitable simulations were available from a broader range of CMIP5 ESMs, we might thus expect the lower end of the

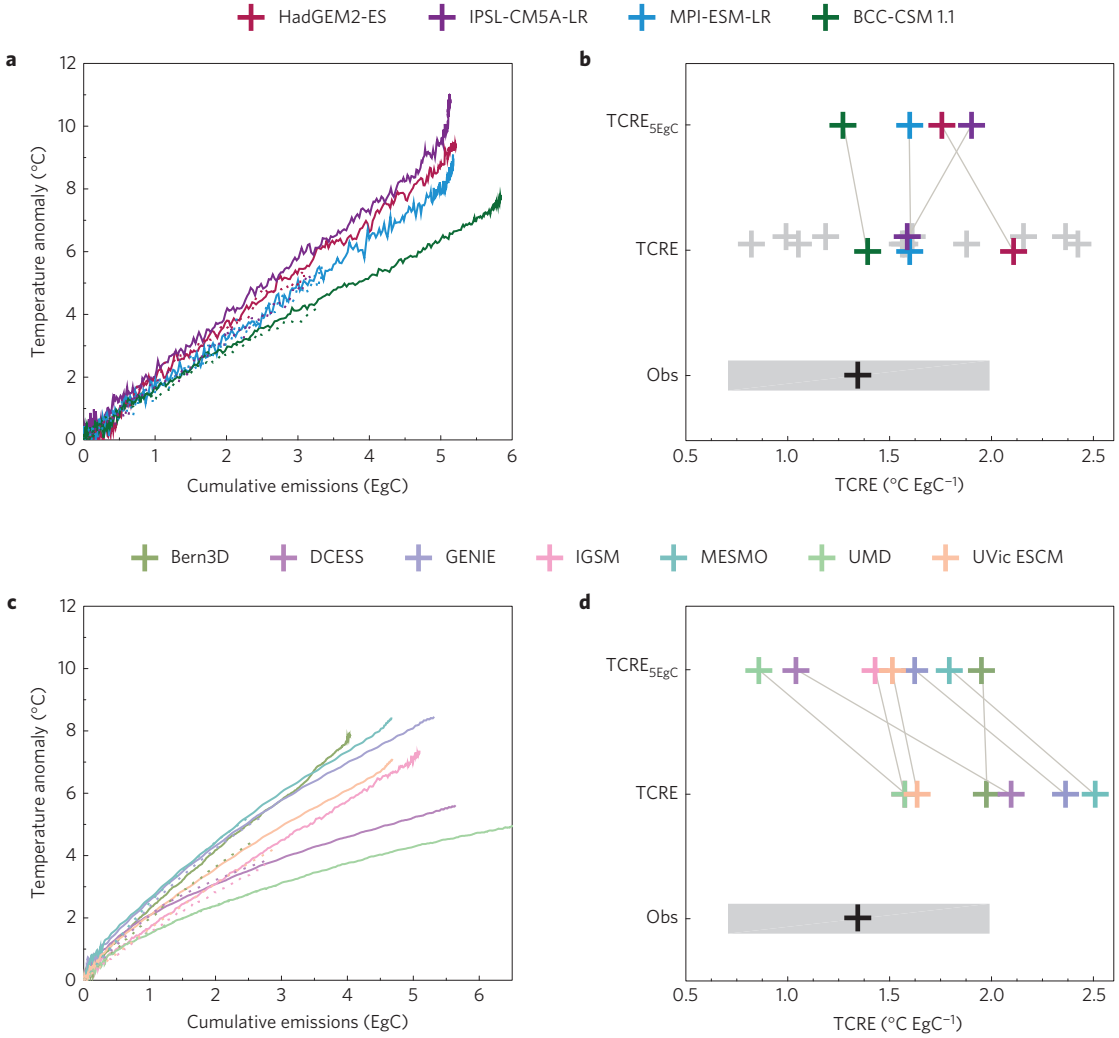

Figure 3 | CO_2-attributable warming as a function of cumulative CO_2 emissions, and the resulting ratio of warming to emissions for CMIP5 ESMs and EMICs. a, Simulated CO_2-attributable warming as a function of cumulative CO_2 emissions based on historical and RCP 8.5-Ext (solid) and 1PCTCO_2 simulations (dotted) from four CMIP5 models. **b**, The ratio of CO_2-attributable warming to cumulative emissions at 5 EgC emissions ($TCRE_{5EgC}$, top row) for these CMIP5 models, compared with TCRE for these models and other CMIP5 models (grey crosses, middle row)[10], and an observationally constrained estimate of TCRE (bottom row)[10]. **c**,**d**, The same as in **a**,**b** but for seven EMICs.

simulated warming at 5 EgC to be extended downwards, but we have no reason to discount the upper end of the warming range simulated by the models we consider on the basis of observational constraints. Accounting for the effects of other forcings as in the RCP 8.5-Ext scenario[12] increases the mean warming at 5 EgC emissions to 9.7 °C (see Methods).

Although the estimated model-mean global mean warming in response to 5 EgC emissions ranges from 6.4 to 9.5 °C, simulated warming considerably exceeds this in some regions, with mean Arctic warming ranging between 14.7 and 19.5 °C (Fig. 4a and Supplementary Fig. 7). Simulated mean changes in precipitation associated with 5 EgC emissions are extremely large (Fig. 4b and Supplementary Fig. 8), with local mean precipitation increases exceeding a factor of four in the tropical Pacific and decreases exceeding a factor of two over parts of Australia, the Mediterranean, southern Africa and the Amazon, and decreases exceeding a factor of three over parts of central America and North Africa. The pattern of temperature and precipitation changes per degree of global mean warming is similar in 2300 to 2100 (Supplementary Fig. 9), and hence is likely to be driven by the same mechanisms[7,27]. Differences between these patterns such as enhanced warming of the high-latitude Southern Hemisphere and relatively larger precipitation increases in 2300 are consistent with the radiative forcing having stabilized near the end of the simulation[7].

In contrast to the results of previous studies using simpler models, we find that in comprehensive ESMs global mean warming increases close to linearly with cumulative carbon emissions even up to five trillion tonnes of carbon emitted, owing to approximately cancelling nonlinear behaviour in the physical climate system and carbon cycle. We suggest that the more linear warming as a function of cumulative emissions in the ESMs compared with the EMICs, which tend to exhibit a reduced rate of warming as cumulative emissions increase, is largely associated with stronger decreases in the efficiency of ocean heat uptake with warming in the ESMs, consistent with other recent studies[22,25], although a more rapid than logarithmic increase in CO_2 radiative forcing or a decline in climate feedback parameter at higher warming levels in the ESMs could also play a role[25]. This implies that the assumption of a constant ratio of warming to cumulative CO_2 emissions is a reasonable assumption for cumulative CO_2 emissions up to 5 EgC, and hence, that proposed policy frameworks based on cumulative CO_2 emissions[4,28,29] are robust over a wide range of plausible CO_2 scenarios. Our results also show that five trillion tonnes of cumulative carbon emissions, corresponding approximately to the unregulated exploitation of the fossil fuel

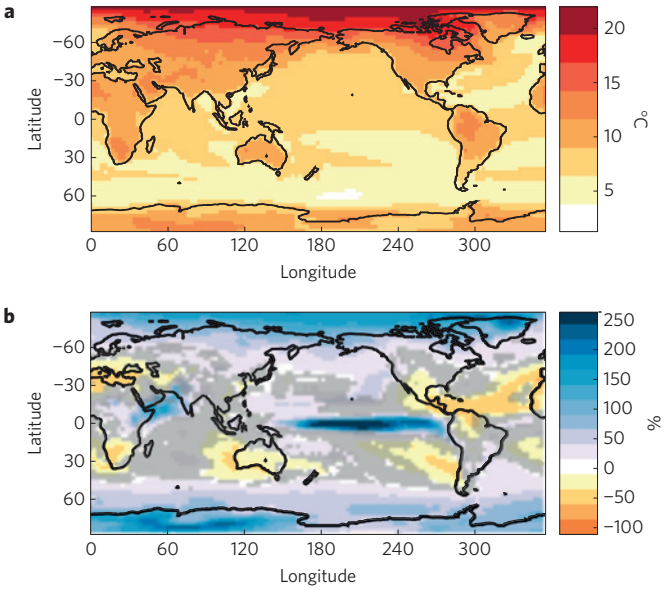

Figure 4 | Simulated model-mean temperature and precipitation changes in response to 5 EgC emissions. a, Multi-model mean temperature change in response to 5 EgC CO_2 emissions, with respect to the pre-industrial control simulation. **b**, Multi-model mean precipitation response to 5 EgC CO_2 emissions, expressed as a percentage of simulated pre-industrial precipitation. The values correspond to the time when cumulative emissions reach 5 EgC, and are scaled by the ratio of CO_2 to total radiative forcing. Grey shading indicates regions of inconsistent model responses, where at least one model shows a change of opposite sign to the model-mean.

resource[4–6], would result in considerably larger global and regional climate changes than previously suggested[8,14]. Such climate changes, if realized, would have extremely profound impacts on ecosystems, human health[30], agriculture, economies and other sectors[24].

Methods

Methods and any associated references are available in the online version of the paper.

Received 29 July 2015; accepted 21 April 2016; published online 23 May 2016

References

1. Friedlingstein, P. *et al*. Persistent growth of CO_2 emissions and implications for reaching climate targets. *Nature Geosci.* **7,** 709–715 (2014).
2. Swart, N. C. & Weaver, A. J. The Alberta oil sands and climate. *Nature Clim. Change* **2,** 134–136 (2012).
3. *Resources to Reserves 2013: Oil, Gas and Coal Technologies for the Energy Markets of the Future* (International Energy Agency, 2013).
4. Moomaw, W. *et al*. in *Climate Change 2001: Mitigation* (eds Pichs-Madruga, R. & Ishitani, H.) Ch. 3 (IPCC, Cambridge Univ. Press, 2001).
5. Cowie, J. *Climate Change: Biological and Human Aspects* (Cambridge Univ. Press, 2013).
6. Henderson-Sellers, A. & McGuffie, K. *The Future of the World's Climate* (Elsevier Science, 2011).
7. Collins, M. *et al*. in *Climate Change 2013: The Physical Science Basis* (eds Stocker, T. F. *et al*.) 1029–1136 (IPCC, Cambridge Univ. Press, 2013).
8. Allen, M. R. *et al*. Warming caused by cumulative carbon emissions towards the trillionth tonne. *Nature* **458,** 1163–1166 (2009).
9. MacDougall, A. H. & Friedlingstein, P. The origin and limits of the near proportionality between climate warming and cumulative CO_2 emissions. *J. Clim.* **28,** 4217–4230 (2015).
10. Gillett, N. P., Arora, V. K., Matthews, D. & Allen, M. R. Constraining the ratio of global warming to cumulative CO_2 emissions using CMIP5 simulations. *J. Clim.* **26,** 6844–6858 (2013).
11. Matthews, H. D., Gillett, N. P., Stott, P. A. & Zickfeld, K. The proportionality of global warming to cumulative carbon emissions. *Nature* **459,** 829–832 (2009).
12. Meinshausen, M. *et al*. The RCP greenhouse gas concentrations and their extensions from 1765 to 2300. *Climatic Change* **109,** 213–241 (2011).
13. Taylor, K. E., Stouffer, R. J. & Meehl, G. An overview of CMIP5 and the experiment design. *Bull. Am. Meteorol. Soc.* **93,** 485–498 (2012).
14. Zickfeld, K. *et al*. Long-term climate change commitment and reversibility: an EMIC intercomparison. *J. Clim.* **26,** 5782–5809 (2013).
15. Arora, V. K. *et al*. Carbon-concentration and carbon-climate feedbacks in CMIP5 Earth system models. *J. Clim.* **26,** 5289–5314 (2013).
16. Friedlingstein, P. *et al*. Uncertainties in CMIP5 climate projections due to carbon cycle feedbacks. *J. Clim.* **27,** 511–526 (2014).
17. Randerson, J. T. *et al*. Multi-century changes in ocean and land contributions to the climate-carbon feedback. *Glob. Biogeochem. Cycles* **29,** 744–759 (2015).
18. Eby, M. *et al*. Historical and idealized climate model experiments: an intercomparison of Earth system models of intermediate complexity. *Clim. Past* **9,** 1111–1140 (2013).
19. Arora, V. K. & Boer, G. J. Terrestrial ecosystems response to future changes in climate and atmospheric CO_2 concentration. *Biogeosciences* **11,** 4157–4171 (2014).
20. MacDougall, A. H., Avis, C. A. & Weaver, A. J. Significant contribution to climate warming from the permafrost carbon feedback. *Nature Geosci.* **5,** 719–721 (2012).
21. Arora, V. K. *et al*. The effect of terrestrial photosynthesis down regulation on the twentieth-century carbon budget simulated with the CCCma Earth System Model. *J. Clim.* **22,** 6066–6088 (2009).
22. Frölicher, T. L. & Paynter, D. J. Extending the relationship between global warming and cumulative carbon emissions to multi-millennial timescales. *Environ. Res. Lett.* **10,** 075002 (2015).
23. Gillett, N. P., Arora, V. K., Zickfeld, K., Marshall, S. J. & Merryfield, W. J. Ongoing climate change following a complete cessation of carbon dioxide emissions. *Nature Geosci.* **4,** 83–87 (2011).
24. IPCC *Climate Change 2014: Impacts, Adaptation, and Vulnerability* (eds Field, C. B. *et al*.) (Cambridge Univ. Press, 2014).
25. Gregory, J. M., Andrews, T. & Good, P. The inconstancy of transient climate sensitivity under increasing CO_2. *Phil. Trans. R. Soc. A* **373,** 20140417 (2015).
26. Herrington, T. & Zickfeld, K. Path dependence of climate and carbon cycle response over a broad range of cumulative carbon emissions. *Earth Syst. Dyn.* **5,** 409–422 (2014).
27. Chadwick, R., Boutle, I. & Martin, G. Spatial patterns of precipitation change in CMIP5: why the rich do not get richer in the tropics. *J. Clim.* **26,** 3803–3822 (2013).
28. IPCC Summary for Policymakers in *Climate Change 2013: The Physical Science Basis* (eds Stocker, T. F. *et al*.) (Cambridge Univ. Press, 2013).
29. Frame, D. J., Macey, A. H. & Allen, M. R. Cumulative emissions and climate policy. *Nature Geosci.* **7,** 692–693 (2014).
30. Sherwood, S. C. & Huber, M. An adaptability limit to climate change due to heat stress. *Proc. Natl Acad. Sci. USA* **107,** 9552–9555 (2010).

Acknowledgements

We thank M. Berkley for assistance in accessing data, and G. Boer and N. Swart for providing comments on the initial version of the manuscript. We acknowledge the World Climate Research Programme's Working Group on Coupled Modelling, which is responsible for CMIP, and we thank the climate modelling groups for producing and making available their model output. For CMIP the US Department of Energy's Program for Climate Model Diagnosis and Intercomparison provides coordinating support and led development of software infrastructure in partnership with the Global Organization for Earth System Science Portals. We acknowledge EMIC AR5 contributors for providing data for EMIC inter-comparison.

Author contributions

N.P.G. and A.J.W. designed the study. K.B.T. collected and analysed data. K.B.T. and N.P.G. interpreted the data and wrote the manuscript. V.K.A. assisted in calculating cumulative carbon emissions and provided manuscript feedback. M.E. assisted in EMIC data analysis and understanding of processes represented by EMICs.

Additional information

Supplementary information is available in the online version of the paper. Reprints and permissions information is available online at www.nature.com/reprints. Correspondence and requests for materials should be addressed to K.B.T.

Competing financial interests

The authors declare no competing financial interests.

Methods

Monthly mean output was taken from 1PCTCO$_2$, historical, RCP 8.5 and RCP 8.5-Ext prescribed CO$_2$ simulations of four CMIP5[13] ESMs that had the data available to calculate cumulative emissions (BCC-CSM1.1, HadGEM2-ES, IPSL-CM5A-LR and MPI-ESM-LR). These are ESMs that include coupled carbon cycles[10]. In the 1PCTCO$_2$ simulations, the atmospheric CO$_2$ concentration increases at a rate of 1% per year for 140 years, starting from the pre-industrial value of approximately 285 ppm (ref. 10). The RCP 8.5-Ext simulations include prescribed concentrations of CO$_2$, other greenhouse gases and aerosols[12], and are continued from the historical simulations. The RCP 8.5-Ext scenarios for the period 2100–2300 are an idealized extension to reach stabilization of radiative forcing at approximately 12 W m^{-2} in year 2300[12].

Cumulative emissions were derived from the prescribed atmospheric CO$_2$ burden and globally integrated monthly mean cumulative atmosphere–ocean and atmosphere–land carbon fluxes. Land-use change emissions estimated for the RCP 8.5-Ext scenario were added separately for all ESM models other than BCC-CSM 1.1[7], in which land-use change was not prescribed. For IPSL-CM5A-LR and BCC-CSM 1.1 models, the cumulative atmosphere–land carbon flux was derived from changes in vegetation, litter and soil carbon pools, because the atmosphere–land carbon flux data were unavailable. For HadGEM2-ES, the atmosphere–land flux data were available only until year 2280; however, the cumulative carbon emissions exceed 5 EgC before that year. The warming and precipitation changes were diagnosed for each model at the time when its respective cumulative carbon emissions reached 5 EgC ($\pm$10 years). Supplementary Table 1 contains the range of estimated warming and years at which each model reaches 5 EgC of cumulative carbon emissions. As the RCP 8.5-Ext simulations include the effects of forcings other than CO$_2$, CO$_2$-attributable warming was estimated by multiplying the total warming by the ratio of CO$_2$ to total forcing in each year. Although a full calculation of the CO$_2$-attributable component of the warming would require separate simulations of the response to RCP 8.5-Ext CO$_2$ changes alone, this is expected to be a good approximation given that the ratio of CO$_2$ to total radiative forcing is approximately constant over the 2150–2300 period and CO$_2$ is the dominant contributor to radiative forcing in the RCP 8.5-Ext scenario (Supplementary Fig. 3). Model mean patterns of temperature and precipitation response at 5 EgC emissions were calculated in a similar way for each model (Supplementary Figs 7 and 8) and then interpolated onto a common grid and averaged.

Globally integrated EMIC temperature and carbon flux data used for comparison with the ESM results were obtained from refs 14,18. For the EMICs that do not reach 5 EgC of cumulative emissions, the TCRE at 5 EgC was calculated using the highest cumulative emissions reached and the corresponding global mean temperature (averaged over a 20-year period).